EXPERIMENTAL STUDY ON CONDENSATION FRICTION PRESSURE DROP IN ROTATING CHANNELS AND PROPOSAL OF NEW CORRELATION

by

Sha WANG, Jixian DONG*, Haozeng GUO, Lijie QIAO, Shulin ZHANG, and Jianyong WANG*

Department of Power Engineering, College of Mechanical and Electrical Engineering,
Shaanxi University of Science and Technology, Xi'an, China

Original scientific paper
https://doi.org/10.2298/TSCI220313111W

The multi-channel cylinder dryer uses the small channels with high heat transfer efficiency to improve the drying efficiency. In practical working conditions, the multi-channel cylinder dryer runs under the rotating state, which would greatly affect the pressure drop of inside two-phase steam. However, the condensation friction pressure drop of two-phase flow in rotating channels has not been well explored. Herein, the condensation pressure drop of two-phase steam in rotating rectangular channels are elaborately studied based on a homemade rotating experiment system. The results show that the friction pressure drop of two-phase flow decreases with the increase of rotation Reynolds number, while increases with the increase of mass flux. Finally, a new correlation of friction pressure drop for two-phase flow condensation in rotating channels is proposed and evaluated by the experimental data.

Key words: *friction pressure drop, two-phase flow condensation, rotating small channel, multi-channel cylinder dryer*

Introduction

The papermaking industry is an important basic industry related to the national economy and social development. As we know, the cylinder dryer is the key part of the dryer section of papermaking machine [1], and it consumes most of the energy that the papermaking process needs. As a result, improving the drying efficiency of cylinder dryer would reduce the energy consumption of papermaking process. The cylinder dryer can be seen as a heat exchanger, in which the high temperature superheated steam flows inside the cylinder and heats the cylinder wall, and then the paper outside the cylinder wall is dried. Therefore, how to enhance the heat transfer effect of cylinder dryer is one of the main ways to improve the drying efficiency of cylinder dryer.

At present, the small channel heat exchanger is one type of the developed heat exchangers with higher heat transfer efficiency, which can effectively increase the heat transfer area of fluids within the finite volume. Hence the small channel heat exchanger is also applied

*Corresponding authors, e-mail: djx@sust.edu.cn, jywang@sust.edu.cn

to the cylinder dryer [2]. A series of small rectangular channels are evenly distributed inside the cylinder wall, making up a multi-channel cylinder dryer (MCD), which is shown in fig. 1. Thus, the steam could flow inside the channels and heat the cylinder wall. The small rectangular channels could not only increase the heat exchange areas, but also break the condensate ring formed during the steam releasing heat and being condensed.

In the existing reference, there are a lot of researches on the fluids flowing in channels, of which some scholars concentrated on the research of condensation pressure drop of fluids in channels. Zhang and Webb [3] used the condensation pressure drop data of multiple working fluids in the small channel to establish a new correlation of friction factor. Wu and Sunden [4] used the existing database to evaluate eleven pressure drop correlations of condensation and evaporation and from which picked out three correlations that are most suitable for the calculation of condensation pressure drop in the micro-channel. Everts and Meyer [5] experimentally studied and compared the relationship between the pressure drop and the heat transfer in a horizontal circular tube under different flow regimes, and the results showed that the pressure drop and the heat transfer can be represented by functions about Grashof number for the laminar flow, while for the other flow states, they can be represented by functions about Reynolds number. Gu *et al*. [6] numerically studied the influence of vapor quality, mass flux and pipe diameter on the condensing pressure drop, and found that the mass flux and vapor quality have a positive effect on pressure drop, while the pipe diameter has a negative effect. Qiao *et al*. [7] studied the pressure drop changes of steam in the MCD under static conditions and the results showed that the separated flow model is more suitable for the condensation pressure drop in the MCD than the homogeneous equilibrium model. Moradkhani *et al*. [8] used the genetic algorithm to fit a model for predicting the frictional pressure drop of fluid condensation in small and micro channels. The obtained model considered some factors including surface tension, inertia, aspect ratio, channel geometry, *etc*.

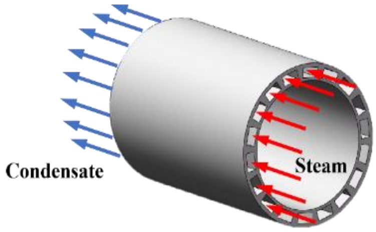

Figure 1. Schematic diagram of MCD

As is known that in actual working conditions, the MCD runs under the rotation state, which would seriously affect the condensation pressure drop of two-phase flow. However, few studies in the literature focused on the condensation pressure drop of fluids in channels under the rotation state. Most investigations about flow characteristic of fluids in rotating channels were concentrated on the turbine blades or thermosiphon pipes. Additionally, it can be seen from the literature review that there was no research exploring the steam condensation pressure drop in rotating channels. Therefore, in this study, an experiment is conducted to investigate the condensation frictional pressure drop of steam flowing in small rectangular channels under rotation states. The experimental results are discussed in detail and a new correlation of condensation pressure drop is proposed finally.

Experimental apparatus and method

Experimental apparatus

The schematic diagram of the experimental apparatus is shown in fig. 2(a). It consists of two parts: the steam circulation system and the coolant circulation system. The coolant circulation system is employed to simulate wet paper. In the steam circulation system, the steam generated by the steam generator enters the steam channel, and then the steam-water mixture flowing out is completely condensed to liquid in the plate heat exchanger and is collected by the water storage tank for recycling. The coolant circulation system uses deionized water as the cooling medium. The cooling water enters the cooling water channel and then takes away the heat released by the steam during the condensation process. The photograph of the experimental apparatus is shown in fig. 2(b).

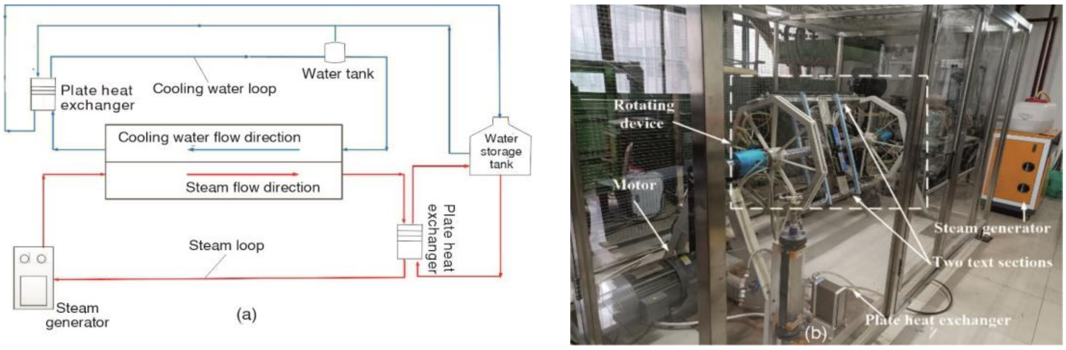

Figure 2. Experimental apparatus; (a) schematic diagram of experimental apparatus and (b) site photo of experimental apparatus

The test sections driven by the rotation device are used to simulate the rotation state of actual dryer. To prevent the vibration resulted from the unbalance of rotating test bench, two test sections are installed symmetrically on the rotating disc. The rotation device has a radius of 400 mm and a length of 1100 mm. According to the previous study [9], the condensate ring is generally formed when the angular velocity reaches 7.04 rad per secund, *i.e*. when the rotation speed reaches 67 rpm, the condensation ring would be formed. The rotation speed is set to 50~100 rpm in this experiment.

Figure 3 shows the details of test section and the measurement point distribution in test section. The test section is mainly composed of a rectangular aluminum plate, on both sides of which some grooves are made as the flow channels. The steam and the cooling water flow in counter-current directions in their respective channels, exchanging heat through the walls. The outside of the channels would be wrapped by rubber thermal insulation material to prevent heat loss.

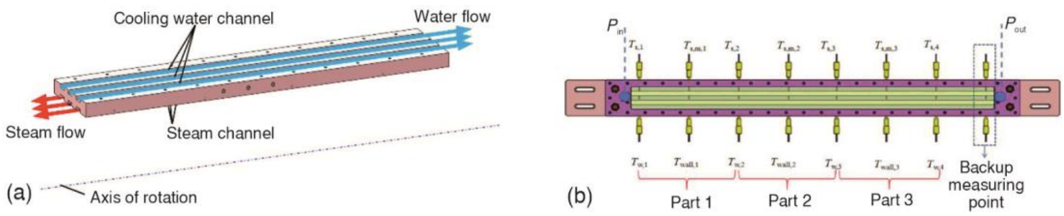

Figure 3. Test section of experimental apparatus; (a) details of test section and (b) measurement point distribution in test section

Two digital pressure sensors with a measurement range of 0-1.6 MPa and a precision of ±0.5% are installed at the inlet and outlet of the steam channels of the test section to measure the steam pressure. Sixteen platinum resistance temperature transducers with a precision of ±0.25% are used to measure the temperature of each part of the channels. The arrangement of sensors and transducers are shown in fig. 3(b). The $T_{s,1}$~$T_{s,4}$ and $T_{s,m,1}$~$T_{s,m,3}$ are steam temperature measuring points, $T_{w,1}$~$T_{w,4}$ are cooling water temperature measuring points, and $T_{wall,1}$~$T_{wall,3}$ are channel wall temperature measuring points. The data collected by the pressure sensors and the temperature transducers are transmitted wirelessly to the computer.

Data processing method

The total pressure drop of fluid in the channel generally consists of several parts that are resulted from including gravity, ΔP_{gr}, acceleration, ΔP_{ac}, friction, ΔP_f, local loss of inlet sudden contraction, ΔP_{in}, and local loss of outlet sudden expansion, ΔP_{out}, as shown:

$$\Delta P_{tp} = \Delta P_{gr} + \Delta P_{ac} + \Delta P_f + \Delta P_{in} + \Delta P_{out} \tag{1}$$

In this study, the gravity pressure drop is not considered because the channels studied here is horizontal. The acceleration pressure drop for condensing flows is calculated [10]:

$$\Delta P_{ac} = \rho \left[\frac{\overline{d\omega}}{dt} \times \vec{r} + \vec{\omega} \times \left(\vec{\omega} \times \vec{r} \right) + 2\vec{\omega} \times \overrightarrow{V_r} \right] \tag{2}$$

where ω is the angular velocity, r – the relative position of fluid particle, and V_r – the relative velocity of fluid.

The local loss of inlet sudden contraction of pressure drop for condensing flows can be calculated [11]:

$$\Delta P_{in} = \left[\frac{G^2 \left(1-\sigma_1\right)}{\sigma_1^2} \right] \left\{ \frac{1+\sigma_1}{2\left(\dfrac{x}{\rho_g} + \dfrac{1-x}{\rho_l} \right)} \left[\frac{x^3}{\rho_g^2 \alpha^2} + \frac{\left(1-x\right)^3}{\rho_l^2 \left(1-\alpha\right)^2} \right] - \sigma_1 \left[\frac{x^2}{\rho_g \alpha} + \frac{\left(1-x\right)^2}{\rho_l \left(1-\alpha\right)} \right] \right\} \tag{3}$$

where G is the steam mass flux, ρ_g – the density of saturated steam, ρ_l – the density of saturated water, x – the vapor quality, σ_1 – the ratio of the cross-sectional area of connecting tube to the inlet cross-sectional area, and α – the void fraction that can be calculated [12]:

$$\alpha = \left[1 + \frac{1-x}{x} \left(\frac{\rho_l}{\rho_g} \right)^{2/3} \right]^{-1} \tag{4}$$

The local loss of outlet sudden expansion of pressure drop for condensing flows is calculated [11]:

$$\Delta P_{out} = \frac{G^2 \left(1-\sigma_2^2\right) \left[\dfrac{x^3}{\rho_g^2 \alpha^2} + \dfrac{\left(1-x\right)^3}{\rho_l^2 \left(1-\alpha\right)^2} \right]}{2\left(\dfrac{x}{\rho_g} + \dfrac{1-x}{\rho_l} \right)} - \frac{G^2 \sigma \left(1-\sigma\right)}{\rho_l} \left[\frac{\left(1-x\right)^2}{\left(1-\alpha\right)} + \left(\frac{\rho_l}{\rho_g} \right) \frac{x^2}{\alpha} \right] \tag{5}$$

where σ_2 is the ratio of the cross-sectional area of connecting tube to the outlet cross-sectional area.

In this study, the friction pressure drop is calculated by eq. (1), of which the total pressure drop is measured by experiment and the others are calculated by eqs. (2)-(5). In the equations, the vapor quality, x, is often used, which are obtained by the following models.

The whole length of channel is divided into 3 parts, as shown in fig. 3(b). In each part, the average quality of vapor is defined as:

$$x_{\mathrm{i}} = \frac{\overline{h_{\mathrm{e,i}}} - h_{\mathrm{l}}}{h_{\mathrm{g}} - h_{\mathrm{l}}} \tag{6}$$

where $\overline{h}_{\mathrm{e,i}}$ is the average specific enthalpy of each part, h_{l} – the specific enthalpy of saturated liquid, and h_{g} – the specific enthalpy of saturated vapour:

$$\overline{h_{\mathrm{e,i}}} = \frac{h_{\mathrm{e,i,in}} + h_{\mathrm{e,i,out}}}{2} \tag{7}$$

where $h_{\mathrm{e,i,in}}$ and $h_{\mathrm{e,i,out}}$ represent the enthalpy of the inlet and outlet of the i^{th} part of channel respectively.

The specific enthalpy of steam at the inlet of the overall channel can be calculated according to the steam temperature and pressure at the inlet:

$$h_{\mathrm{e,in}} = f\left(t_{\mathrm{s,in}}, P_{\mathrm{s,in}}\right) \tag{8}$$

where $t_{\mathrm{s,in}}$, $P_{\mathrm{s,in}}$, $h_{\mathrm{e,in}}$ are the temperature, pressure, and specific enthalpy of steam at the inlet of channel respectively.

The exterior of all experimental sections is almost thermal insulated, so the heat loss to the environment can be ignored in the calculation. According to the energy balance of the condensation heat transfer of steam in the channel:

$$Q_{\mathrm{s,i}} = Q_{\mathrm{w,i}} \tag{9}$$

where $Q_{\mathrm{s},i}$ is the heat released by steam condensation in one part and $Q_{\mathrm{w},i}$ – the heat absorbed by cooling water in one part.

The calculation formula for the heat absorbed by cooling water is:

$$Q_{\mathrm{w,i}} = c_p \dot{m}_{\mathrm{w}} \left(T_{\mathrm{w,i+1}} - T_{\mathrm{w,i}}\right) \tag{10}$$

where c_p is the specific heat capacity of cooling water, $\dot{m}_{\mathrm{w}}$ – the mass flow rate of cooling water, and $t_{\mathrm{w,i+1}}$ and $t_{\mathrm{w,i}}$ – the outlet temperature and inlet temperature of cooling water of each part measured by the resistance thermometers.

Hence the specific enthalpy of steam at the outlet of each part is:

$$h_{\mathrm{e,i+1}} = h_{\mathrm{e,i}} + \frac{c_p \dot{m}_{\mathrm{w}} \left(T_{\mathrm{w,i+1}} - T_{\mathrm{w,i}}\right)}{\dot{m}_{\mathrm{s}}} \tag{11}$$

where $\dot{m}_{\mathrm{s}}$ is the mass flow of steam.

In addition, the rotation Reynolds number, Re_{ω}, characterizes the ratio of Coriolis force to viscous force:

$$\mathrm{Re}_{\omega} = \frac{\omega D_{\mathrm{h}}^2}{\nu} \tag{12}$$

where ω is the rotational angular velocity, ν – the kinematic viscosity of fluid, and D_{h} – the hydraulic Diameter of the channel.

Uncertainty analysis

In this paper, the uncertainty calculation method in [13] is used to evaluate the possible uncertainty of experimental results, and the calculation results are shown in tab. 1. It can be seen that the maximal uncertainty of pressure drop is ±3.6%, which indicates that the calculation results in this article are considered reliable.

Table 1. Uncertainty analysis results

Parameter	Steam temperature [°C]	Cooling water temperature [°C]	Wall temperature [°C]	Steam mass flux [kgm^{-2}s^{-1}]	Pressure drop [kPa]
Range	±0.77%	±0.77%	±0.77%	±0.95%	±3.6%

Results and discussion

In this section, the reliability of the experimental apparatus is verified firstly. Then the effects of rotation speed and mass flux on the pressure drop of steam in the channel are experimentally studied. In addition, the experimental results are compared with some results calculated by the pressure drop correlations in the reference. Finally, a new correlation for the condensation pressure drop of steam in rotating channels is proposed and evaluated by the experimental data.

Reliability verification of experimental apparatus

In order to verify the reliability of experimental apparatus, an experiment for condensation pressure drop of steam in static channels was conducted, and then a data comparison between the results of the above experiment and the results calculated by a classic correlation was performed. The correlation proposed by Kim *et al*. [14], which is used to predict the condensation pressure drop in rectangular tubes, was employed here. As for the previous experiment, the mass flux is in the range of 50~80 kg/m^{2}s and the steam temperature is 120 °C. Figure 4 shows the comparison results. It can be seen that the error of most data are within 20%, indicating the reliability of the experimental apparatus:

$$C=\left\{\begin{array}{l}0.39\,\mathrm{Re}_{\mathrm{lo}}^{0.03}\,\mathrm{Su}_{\mathrm{go}}^{0.10}\left(\dfrac{\rho_\mathrm{l}}{\rho_\mathrm{g}}\right)^{0.35} \ldots\left(\mathrm{Re}_\mathrm{l}\geq 2000,\ \mathrm{Re}_\mathrm{g}\geq 2000\right)\\ 8.7\times 10^{-4}\,\mathrm{Re}_{\mathrm{lo}}^{0.17}\,\mathrm{Su}_{\mathrm{go}}^{0.50}\left(\dfrac{\rho_\mathrm{l}}{\rho_\mathrm{g}}\right)^{0.14} \ldots\left(\mathrm{Re}_\mathrm{l}\geq 2000,\ \mathrm{Re}_\mathrm{g}\geq 2000\right)\\ 0.0015\,\mathrm{Re}_{\mathrm{lo}}^{0.59}\,\mathrm{Su}_{\mathrm{go}}^{0.19}\left(\dfrac{\rho_\mathrm{l}}{\rho_\mathrm{g}}\right)^{0.36} \ldots\left(\mathrm{Re}_\mathrm{l}\geq 2000,\ \mathrm{Re}_\mathrm{g}\geq 2000\right)\\ 3.5\times 10^{-5}\,\mathrm{Re}_{\mathrm{lo}}^{0.44}\,\mathrm{Su}_{\mathrm{go}}^{0.50}\left(\dfrac{\rho_\mathrm{l}}{\rho_\mathrm{g}}\right)^{0.48} \ldots\left(\mathrm{Re}_\mathrm{l}\geq 2000,\ \mathrm{Re}_\mathrm{g}\geq 2000\right)\end{array}\right\} \tag{13}$$

where $\mathrm{Re}_{\mathrm{lo}}$, $\mathrm{Re}_{\mathrm{go}}$ are liquid or gas only Reynolds number and Re_l, Re_g are superficial liquid or gas Reynolds number:

$$\mathrm{Re}_{\mathrm{lo}}=\frac{GD_\mathrm{h}}{\mu_\mathrm{l}} \tag{14}$$

$$\mathrm{Re}_{\mathrm{go}}=\frac{GD_\mathrm{h}}{\mu_\mathrm{g}} \tag{15}$$

$$\mathrm{Re}_\mathrm{l}=\frac{GD_\mathrm{h}}{\mu_\mathrm{l}}(1-x) \tag{16}$$

$$\mathrm{Re_g} = \frac{GD_\mathrm{h}}{\mu_\mathrm{g}} x \tag{17}$$

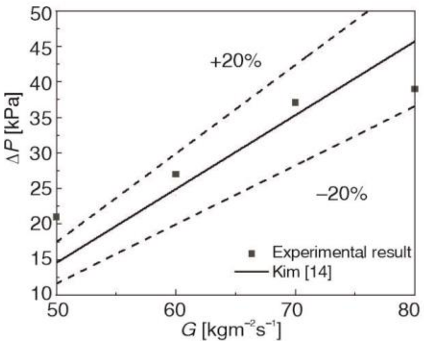

Figure 4. Comparison of experimental result with Kim correlation for rectangular channel

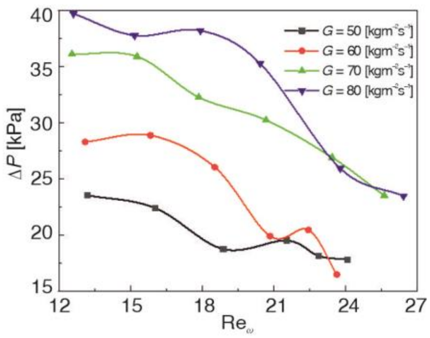

Figure 5. Effect of Re_ω on friction pressure drop

Experimental results

In the experiment, the rotation speed is 50~100 rpm, the mass flux, G, is 50~80 kg/m^{2}s, the steam temperature is 120 °C, and the hydraulic diameter is 6.75 mm, hence Re_ω approximately ranges from 12 to 27 according to eq. (12). The influence of Re_ω on frictional pressure drop is shown in fig. 5. It can be seen that the frictional pressure drop decreases significantly as Re_ω increases. For example, when the G is 70 kg/m^{2}s, the friction pressure drops from 28.28 to 16.48 kPa as Re_ω rises from 12 to 26. The rate of steam forming condensate increases with the rotation speed. The steam quality decreases as the steam flows in the channel, resulting in an increase in the liquid phase velocity and a decrease in the gas phase velocity, hence the velocity difference between the two phases is reduced, leading to the frictional pressure drop decreasing. On the other hand, due to the big density difference between the gas and liquid phases, the stratification effect is produced by rotation, which reduces the obstruction of the liquid phase to the gas phase. Therefore, when Re_ω increases, the friction pressure drop of the two-phase flow decreases.

Figure 5 also shows that the mass flux has a positive impact on the friction pressure drop at the same Re_ω. The present data are similar to the effect of mass flux on the friction pressure drop under static conditions [15]. For example, when Re_ω is 13, the friction pressure drop increases from 23.54 to 39.69 kPa as the mass flux rises from 50 to 80 kg/$^{-2}$s. In addition, the friction pressure drop decreases slowly when the Re_ω is small. Since the flow rate of the two-phase increases when the mass flux increases, the friction between the steam and the condensate increases, and so does the friction between the condensate and the channel wall.

Correlations comparison

In this experiment, the steam is condensed and releases heat in the rotating rectangular channels. The density of steam and condensate are very different, and the centrifugal force on the steam and condensate are also different, so the two-phase fluid cannot be uniformly mixed. At the same time, some scholars have proved that the homogeneous models are not suitable for the condition of mass fluxes lower than 2000 kg/m^{2}s [16]. Therefore, in this section, a separated flow model is used to predict the frictional pressure drop in the channel. Eight correlations of two-phase frictional pressure drop are summarized in tab. 2.

Table 2 Correlations for friction pressure drop

Models	Correlations	Applicable conditions
[17]	$\left(\frac{\mathrm{d}p}{\mathrm{d}z}\right)_\mathrm{f} = \left(\frac{\mathrm{d}p_\mathrm{f}}{\mathrm{d}z}\right)_\mathrm{l} \Phi_\mathrm{l}^2, \quad \Phi_\mathrm{l}^2 = 1 + \frac{C}{X} + \frac{1}{X^2}$ where C is the constant and X is the Martinelli parameter	$1.49 < D_\mathrm{h} < 25.83$ mm
[18]	$C + 21\left(1 - \mathrm{e}^{0.319 D_\mathrm{h}}\right)$	$1 < D_\mathrm{h} < 4$ mm
[19]	$C = 4.6468 \times 10^{-6} \left(\frac{P}{P_\mathrm{crit}}\right)^{5.586} \mathrm{Re}_\mathrm{l}^{0.4387} \left(\frac{\rho_\mathrm{l}}{\rho_\mathrm{g}}\right)^{5.7189} X^{-0.4243}$	Rectangular duct $D_\mathrm{h} = 1.16$ mm
[14]	If $Re_\mathrm{l} \geq 2000$, $Re_\mathrm{g} \geq 2000$ $C = 0.39 \mathrm{Re}_\mathrm{fo}^{0.03} \mathrm{Su}_\mathrm{go}^{0.10} \left(\frac{\rho_\mathrm{l}}{\rho_\mathrm{g}}\right)^{0.35}$ If $Re_\mathrm{l} \geq 2000$, $Re_\mathrm{g} < 2000$ $C = 8.7 \times 10^{-4} \mathrm{Re}_\mathrm{fo}^{0.07} \mathrm{Su}_\mathrm{go}^{0.5} \left(\frac{\rho_\mathrm{l}}{\rho_\mathrm{g}}\right)^{0.14}$ If $Re_\mathrm{l} < 2000$, $Re_\mathrm{g} \geq 2000$ $C = 0.0025 \mathrm{Re}_\mathrm{fo}^{0.59} \mathrm{Su}_\mathrm{go}^{0.19} \left(\frac{\rho_\mathrm{l}}{\rho_\mathrm{g}}\right)^{0.36}$ If $Re_\mathrm{f} < 2000$, $Re_\mathrm{g} < 2000$ $C = 3.5 \times 10^{-5} \mathrm{Re}_\mathrm{fo}^{0.44} \mathrm{Su}_\mathrm{go}^{0.5} \left(\frac{\rho_\mathrm{l}}{\rho_\mathrm{g}}\right)^{0.48}$	Single and multi-port tubes $0.0695 < D_\mathrm{h} < 6.22$ mm
[20]	$\left(\frac{\mathrm{d}p}{\mathrm{d}z}\right)_\mathrm{f} = \left(\frac{\mathrm{d}p_\mathrm{f}}{\mathrm{d}z}\right)_\mathrm{lo} \Phi_\mathrm{lo}^2, \quad \Phi_\mathrm{lo}^2 = 1 + \left(Y^2 - 1\right)\left\{B\left[x(1-x)\right]^{0.875} + x^{1.75}\right\}$ B is the empirical coefficient and Y is the Chisholm parameter	
[21]	$\left(\frac{\mathrm{d}p}{\mathrm{d}z}\right)_\mathrm{f} = \left(\frac{\mathrm{d}p_\mathrm{f}}{\mathrm{d}z}\right)_\mathrm{g} \Phi_\mathrm{g}^2, \quad \Phi_\mathrm{g}^2 = 1 + CX_\mathrm{tt}^\mathrm{n} + X_\mathrm{tt}^2$ $X_\mathrm{tt} = \left(\frac{1-x}{x}\right)^{0.9} \left(\frac{\rho_\mathrm{g}}{\rho_\mathrm{l}}\right)^{0.5} \left(\frac{\mu_\mathrm{l}}{\mu_\mathrm{g}}\right)^{0.1}, \quad C = 21\left(1 - \mathrm{e}^{0.28\mathrm{Bo}^{0.5}}\right)\left[2 - 1.9\mathrm{e}^{\left(-0.016\mathrm{Fr}^{1.4}\right)}\right]$	Round tube $D_\mathrm{h} = 4.35$ mm
[22]	$\Phi_\mathrm{l}^2 = 1 + \frac{C}{X^{1.19}} + \frac{1}{X^2}, \quad C = 1.79\left(\frac{\mathrm{Re}_\mathrm{g}}{\mathrm{Re}_\mathrm{l}}\right)^{0.4}\left(\frac{1-x}{x}\right)^{0.5}$	Single and multi-port tubes. $0.506 < D_\mathrm{h} < 12$ mm
[23]	$\left(\frac{\mathrm{d}p}{\mathrm{d}z}\right)_\mathrm{f} = \left(\frac{\mathrm{d}p_\mathrm{f}}{\mathrm{d}z}\right)_\mathrm{lo} \Phi_\mathrm{lo}^2$ $\Phi_\mathrm{lo}^2 = 12.82(1-x)^{1.8} + X_\mathrm{tt}^{-1.47}, \quad X_\mathrm{tt} = \left(\frac{1-x}{x}\right)^{0.9}\left(\frac{\rho_\mathrm{g}}{\rho_\mathrm{l}}\right)^{0.5}\left(\frac{\mu_\mathrm{l}}{\mu_\mathrm{g}}\right)^{0.1}$	Single and multi-port tubes

The Lockhart-Martinelli (L-M) [17] correlation is proposed in the early period to conduct experimental research on the flow of benzene, kerosene, water, and air in a pipe with an inner diameter of 1.5-25.8 mm. The three correlations including Mishima and Hibiki [18], Lopez-Belchi [19], and Kim [14] are all modified based on the L-M correlation. The L-M correlation does not consider the interaction force between the two phases. To study the influence of pipe diameter on frictional pressure drop, Mishima and Hibiki [18] experimentally researched the friction pressure drop of different fluids in round and square pipes, then compared the experimental results with the L-M correlation, and finally modified the parameter, *C*. The new correlation shows that the deviation of the calculation results of steam condensation with the experimental results is within 25%. Lopez-Belchi *et al*. [19] used a variety of refrigerants to analyze the influence of mass flux and vapor quality on the condensing friction pressure drop in a rectangular channel. Then the ratio of the inertial force to the viscous force and the change of the fluid properties with the saturation temperature is added to the parameter, *C*, of correlation for fitting. The average relative deviation of the new correlation is 9.51%. Meanwhile, the new correlation shows the best prediction for condensation flow with values of 17.5%.

The Chisholm [20] correlation successfully correlates the pressure drop with pressure, mass flux, vapor quality, and physical properties of working fluid. It is not only suitable for water-steam systems but also for other types of two-phase fluids. Hossain *et al*. [21] studied the condensation pressure drop in a circular tube with an inner diameter of 4.35 mm under different mass velocity and refrigerant conditions. This model considers the influence of mass velocity and surface tension, then uses the Bond number and Froude number as variables for the parameter, *C*. Sun and Mishima [22] found that *C* is affected not only by Suratman number but also by the ratio of Re_g to Re_l, then the Chisholm correlation is modified. The mean error of the new correlation is 22.21%. Wilson *et.al*. [23] proved the error of the condensation pressure drop of the refrigerant in the flat tube is within 40% through experiment.

The absolute relative deviation MARD is used to predict the accuracy of each pressure drop correlation. The calculation formula of MARD is shown:

$$MARD = \frac{1}{N}\sum_{i-1}^{N}\left|\frac{\left(\frac{\mathrm{d}p}{\mathrm{d}z}\right)_{(i)\mathrm{pred}} - \left(\frac{\mathrm{d}p}{\mathrm{d}z}\right)_{(i)\exp}}{\left(\frac{\mathrm{d}p}{\mathrm{d}z}\right)_{(i)\exp}}\right| \tag{18}$$

where the subscripts pred and exp denote the predicted value and experimental value, respectively.

Figure 6 presents the comparison of frictional pressure drop calculated by the aforementioned correlations with the experimental data. It can be seen that, compared with other correlations, the Chisholm [20] and Wilson *et al*. [23] correlations have the lowest prediction accuracy. These two correlations completely overpredict the frictional pressure drop in the rotating rectangular channel at different mass flux.

The Hossain *et al*. [21], Mishima and Hibiki [18], and Lopez-Belchi [19] correlations all underpredict the frictional pressure drop of two-phase flow in the rotating rectangular channel. The hydraulic diameters of these three correlations are slightly smaller than the experimental results. The absolute error of Mishima and Hibiki [18] correlation is 41.2%, and moreover 77.7% of the data are outside the 30% error band, which is resulted from that this correlation uses water or air as working fluid. The absolute errors of Hossain *et al*. [21] and Lopez-Belchi [19] correlations are 31.4% and 39.4%, respectively, compared with the experimental data. These two correlations use different refrigerants (R1234yf, R134a, R32, and R410A, *etc*.) as the medium.

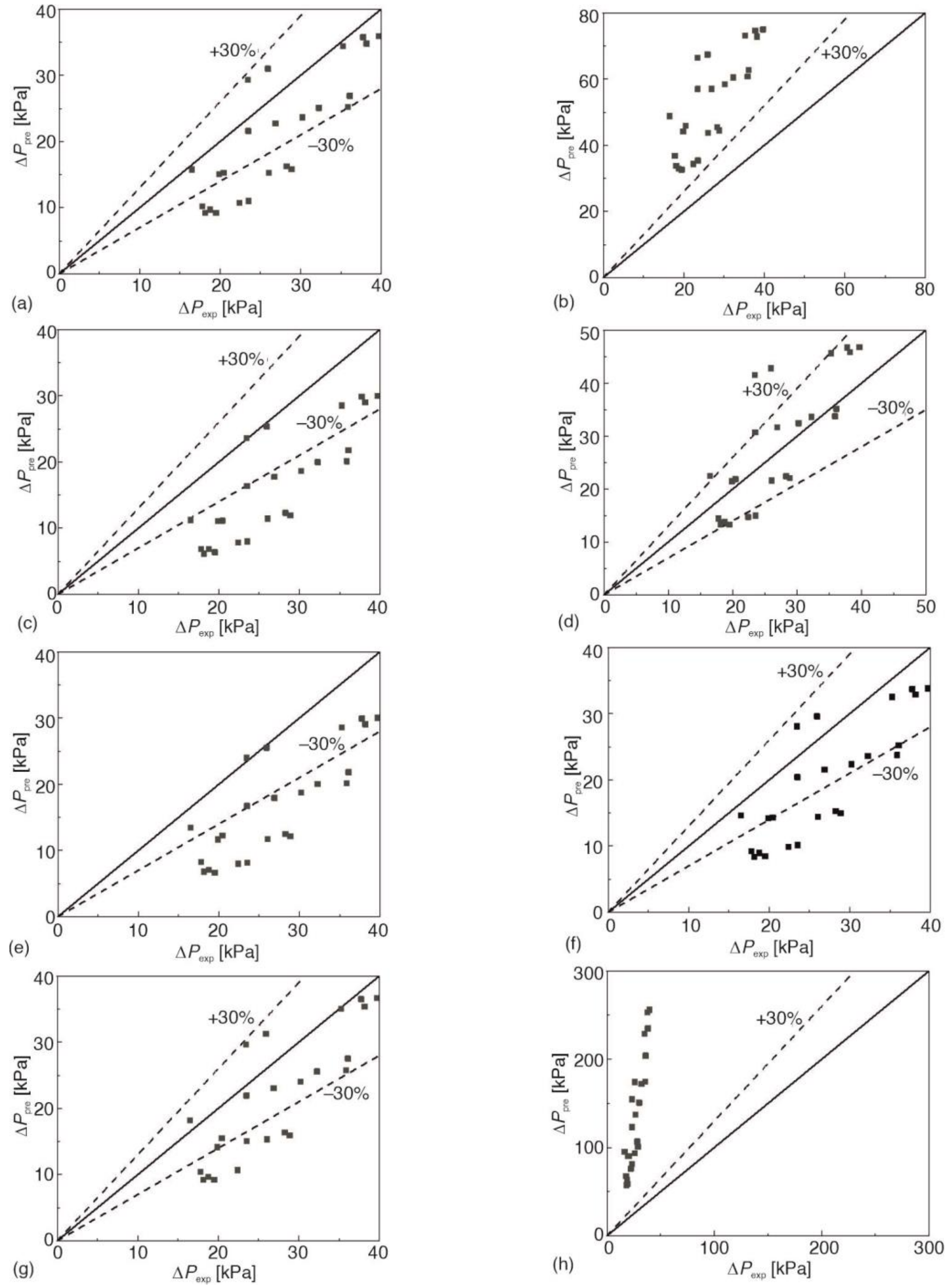

Figure 6. Comparison of experimental results with some related correlations; (a) L-M [17], (b) Chisholm [20], (c) Mishima and Hibiki [18], (d) Kim [14], (e) Lopez-Belchi [19], (f) Hossain *et al*. [21], (g) Sun and Mishima [22], and (h) Wilson *et al*. [23]

The L-M [17] and Sun and Mishima [22] correlations slightly underpredict experimental data. Both models have a relatively large range of hydraulic diameters, including the hydraulic diameter in this experiment. Compared with the experimental data, the absolute error of L-M [17] is equal to 27.7%, and 59.2% of the data points are within the 30% error band. The absolute error of Sun and Mishima [22] is 27%, and 59% of the data points are within the 30% error band.

The Kim *et al*. [14] correlation provides the best predictions, and its calculation method is also the most complicated. Compared with the experimental data, the absolute error is 25%, and 70.4% of the data are within the 30% error band. The hydraulic diameter of Kim *et al*. [14] ranges from 0.0695-6.22 mm, which is most close to the hydraulic diameter of the channel in this experiment. The Kim *et al*. [14] correlation uses 7115 data to divide the two-phase flow pattern into four areas, and then modifies, *C*, in the four areas. The model is suitable for a wide range of working fluids with a wide range of hydraulic diameters and mass flux, while taking into account the thermophysical properties of the fluid.

Proposal of new correlation

As previously analyzed, all the existing correlations cannot accurately predict the friction pressure drop for condensing flows in the rotating channel. Therefore, a new high-precision prediction correlation needs to be proposed.

The new correlation is modified based on the L-M correlation and meanwhile considers the influence of rotation on the pressure drop in the small channel. In particular, the influence of the pressure drop in the rotating small channel is represented by a dimensionless parameter, which replaces the constant, *C*, in the L-M correlation.

At the rotation state, the pressure drop must consider the effects of inertia and viscous forces, and the interaction between the liquid and the gas phases also affects the pressure drop. Therefore, the dimensionless parameters include rotation Reynolds number, Reynolds number, and Suratman number. The density ratio is introduced to consider the influence of different working fluids.

The Suratman number, $\mathrm{Su_{go}}$, can be defined as:

$$\mathrm{Su_{go}} = \frac{\rho_\mathrm{g} \sigma D_\mathrm{h}}{\mu_\mathrm{g}^2} \tag{19}$$

Considering the aforementioned factors that influence the friction pressure drop and based on the existing friction pressure drop correlation, a new correlation related to the non-dimensional parameters including $\mathrm{Re_{lo}}$, $\mathrm{Re_\omega}$, and $\mathrm{Su_{go}}$ is proposed:

$$C = a \mathrm{Re}_\mathrm{lo}^b \mathrm{Re}_\omega^c Su_\mathrm{go}^d \left(\frac{\rho_\mathrm{l}}{\rho_\mathrm{g}}\right)^e \tag{20}$$

where *a, b, c, d,* and *e* are coefficients.

Based on this analysis, a prediction calculation is conducted with BP neural network algorithm, and five parameters are selected including temperature, rotation speed, pressure, viscosity and density. Through the training with more than six hundred sets of data, the fitting formula is derived. The non-dimensional coefficients are obtained as shown in tab. 3. It can be seen that the correlation is divided into three parts according to the ratio of $\mathrm{Re_l}$ to $\mathrm{Re_g}$. The comparison between the fitting results of the new correlation and the 200 experimental data is shown in fig. 7.

Table. 3 Non-dimensional coefficient results

Re_l/Re_g	*a*	*b*	*c*	*d*	*e*
$Re_l/Re_g > 0.02$	4.043	0.196	0.462	0.001	–0.063
$0.008 < Re_l/Re_g \leq 0.02$	–0.484	0.308	0.074	0.007	0.143
$Re_l/Re_g \leq 0.08$	–16.641	0.376	0.471	–0.36	0.238

It can be seen that the friction pressure drop calculated by the new correlation is basically consistent with the experimental data. The average deviation of new correlation is 17.5% and moreover 85% of the data are inside the 30% error band. Therefore, the proposed correlation can well predict the friction pressure drop of steam condensation in the rotating rectangular channel.

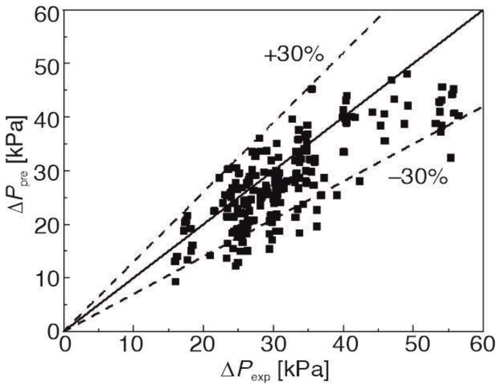

Figure 7. Comparison of experimental results with proposed new correlation

Conclusion

In this paper, the friction pressure drop of steam condensation in the rotating rectangular channel is investigated. Firstly, the experimental apparatus is described in detail and its reliability is verified. Then the effects of rotating speed and mass flux on the pressure drop of steam condensation in the rotating channel are experimentally studied. The experimental results are compared with some results calculated by the pressure drop correlations in the reference. Finally, a new correlation for the friction pressure drop of two-phase flow condensation in rotating channels is proposed and evaluated by the experimental data. Some main conclusions are obtained as follows.

- The pressure drop of the two-phase flow in the rotating channel decreases with the increase of Re_ω. When Re_ω is constant, the friction pressure drop increases as the steam mass flux increases. When the Re_ω is small, the friction pressure drop decreases slowly under the condition of same steam mass flux.
- The experimental data are compared with the eight existing two-phase flow friction pressure drop correlations. Among the eight correlations of predicting the pressure drop in small and micro channels, the Kim *et al.* [14] correlation is most suitable for the experimental data, but the absolute error is still 25% and only 70.4% of the data points are within the 30% error band.
- A new correlation, which considers three dimensionless parameters and the density ratio of liquid to gas, is proposed to predict friction pressure drop of condensing two-phase flow in rotating channels. The research results show that the deviations between the calculation results by the new correlation and the experimental data are mostly within 30%, and the average deviation is only 17.5%.

Funding

The study is supported by National Natural Science Foundation of China (Grant No. 51906131 and No. 51375286) and Natural Science Fundamental Research Program of Shaanxi Province (Grant No. 2020CGHJ-025).

Nomenclature

a-e	– coefficient
Bo	– Bond number
c_p	– specific heat capacity, [$\mathrm{Jkg^{-1}K^{-1}}$]
D_h	– hydraulic diameter
G	– mass flux, [$\mathrm{kgm^{-2}s^{-1}}$]
h_e	– specific enthalpy,[$\mathrm{Jkg^{-1}}$]
h_g	– specific enthalpy of saturated vapor, [$\mathrm{Jkg^{-1}}$]
h_l	– specific enthalpy of saturated liquid, [$\mathrm{Jkg^{-1}}$]
$\dot{m}$	– mass-flow rate, [$\mathrm{kgs^{-1}}$]
P	– pressure, [Pa]
P_crit	– critical pressure
Q	– thermal power, [W]
Re	– Reynolds number
Re_ω	– rotation Reynolds number
r	– relative position of fluid particle
Su	– Suratman number
T	– temperature, [K]
V_r	– velocity of the fluid, [$\mathrm{ms^{-1}}$]
X	– Martinelli parameter
x	– vapor quality

Greek symbols

α	– thermal diffusivity, [$\mathrm{m^2s^{-1}}$]
β	– volume expansion coefficient, [K]
μ	– dynamic viscosity, [Pa s]
ν	– kinematic viscosity, [$\mathrm{m^2s^{-1}}$]
ρ	– density, [$\mathrm{kgm^{-3}}$]
σ	– cross-sectional area
Φ	– friction factor
ω	– rotational velocity, [$\mathrm{rads^{-1}}$]

Subscript

ac	– acceleration
exp	– experiment
f	– friction
g	– gas
go	– gas only
gr	– gravity
i	– i^th part of channel
in	– inlet
l	– liquid
lo	– liquid only
m	– middle
out	– outlet
pre	– predicted
s	– steam
tp	– two-phase
wall	– wall
w	– cooling water

References

[1] Yan, Y., *et al.*, Condensation Heat Transfer Characteristics and Flow Regime in a Horizontal Rectangle Channel of a Multi-Channel Cylinder Dryer, *Drying Technology*, *36* (2017), 11, pp. 122-123

[2] Shina, J. H., *et al.*, Flow and Thermal Characteristics of Condensing Steam in a Single Horizontal Mini-Channel of a Multiport Cylinder Dryer, *Drying Technology*, *29* (2010), 1, pp. 47-54

[3] Zhang., M., Webb, R. L., Correlation of Two-Phase Friction for Refrigerants in Small-Diameter Tubes, *Experimental Thermal and Fluid Science*, *25* (2001), 3-4, pp. 131-139

[4] Wu, Z., Sunden, B., Frictional Pressure Drop Correlations for Single-Phase Flow, Condensation, and Evaporation in Microfin Tubes, *Journal of Heat Transfer*, *138* (2016), 2, pp. 022901-1-022901-9

[5] Everts, M., Meyer, J. P., Relationship Between Pressure Drop and Heat Transfer of Developing and Fully Developed Flow in Smooth Horizontal Circular Tubes in the Laminar, Transitional, Quasi-Turbulent and Turbulent Flow Regimes, *International Journal of Heat Mass Transfer*, *117* (2018), Feb., pp. 1231-1250

[6] Xin, G., *et al.*, Condensation Flow Patterns and Model Assessment for R1234ze(E) in Horizontal Mini/Macro-Channels, *International Journal of Thermal ences*, *134* (2018), Dec., pp. 140-159

[7] Qiao, L., *et al.*, Heat Transfer Characteristics in Horizontal Rectangular Channel of Multi-Channel Cylinder Dryer, *Palpu Chongi Gisul/Journal of Korea Technical Association of the Pulp Paper Industry*, *52* (2020), 3, pp. 77-89

[8] Moradkhani, M.A., *et al.*, A General Correlation for the Frictional Pressure Drop During Condensation in Mini/Micro and Macro Channels, *International Journal of Heat Mass Transfer*, *163* (2020), 120475

[9] Shu, Q., Experimental Study and Numerical Simulation of Condensate Motion and Heat Transfer Within Paper Machine Dryer Section, Ph. D. thesis, Shaanxi University of Science & Technology, Xi'an, China, 2009

[10] Zhang, J., *et al.*, Characteristics of Pressure Drop and Correlation of Friction Factors for Single-Phase Flow in Rolling Horizontal Pipe, *Journal of Hydrodynamics Ser B*, *21* (2009), 5, pp. 614-621

[11] Lin, Z., *Gas-Liquid Two-Phase Flow and Boiling Heat Transfer*, Xi'an Jiaotong University Press, Xi'an, China, 1987

[12] Rohsenow, W. M., *et al.*, *Handbook of Heat Transfer*. Osborne McGraw-Hill, New York, USA, 1973

[13] Robert, J. M., *et al.*, Describing the uncertainties in experimental results, *Experimental Thermal Fluid Science*, *1* (1988), 1, pp. 3-17
[14] Kim, S. M., Mudawar, I., Universal Approach to Predicting Two-Phase Frictional Pressure Drop for Adiabatic and Condensing Mini/Micro-Channel Flows, *International Journal of Heat Mass Transfer*, *55* (2012), 11-12, pp. 3246-3261
[15] Yoo, J. W., *et al.*, Experimental Study of Propane Condensation Heat Transfer and Pressure Drop in Semicircular Channel Printed Circuit Heat Exchanger, *International Journal of Heat and Mass Transfer*, *182* (2022), 121939
[16] Rahman, M.M., *et al.*, Comparison and Development of New Correlation for Adiabatic Two-Phase Pressure Drop of Refrigerant Flowing Inside a Multiport Minichannel with and Without Fins, *International Journal of Refrigeration*, *82* (2017), Oct., pp. 119-129
[17] Lockhart, R. W., Martinelli, R. C., Proposed Correlation of Data for Isothermal Two-Phase, Two-Component Flow in Pipes, *Chem.eng.prog*, *45* (1949), 1, pp. 39-48
[18] Mishima, K., Hibiki, T., Some Characteristics of Air-Water Two-Phase Flow in Small Diameter Vertical Tubes, *International Journal of Multiphase Flow*, *22* (1996), 4, pp. 703-712
[19] Lopez-Belchi, A., *et al.*, Experimental Condensing Two-Phase Frictional Pressure Drop Inside Mini-Channels. Comparisons and New Model Development, *International Journal of Heat Mass Transfer*, *75* (2014), Aug., pp. 581-591
[20] Chisholm, D., Pressure Gradients due to Friction During the Flow of Evaporating Two-Phase Mixtures in Smooth Tubes and Channels, *International Journal of Heat Mass Transfer*, *16* (1973), 2, pp. 347-358
[21] Hossain, M.A., *et al.*, Two-phase Frictional Multiplier Correlation for the Prediction of Condensation Pressure Drop Inside Smooth Horizontal Tube, *Procedia Engineering*, *105* (2015), Dec., pp. 64-72
[22] Sun, L., Mishima, K., Evaluation analysis of prediction methods for two-phase flow pressure drop in mini-channels, *International Journal of Multiphase Flow*, *35* (2009), 1, pp. 47-54
[23] Wilson, M. J., *et al.*, Refrigerant Charge, Pressure Drop, and Condensation Heat Transfer in Flattened Tubes, *International Journal of Refrigeration*, *26* (2003), 4, pp. 442-451

Paper submitted: March 13, 2022
Paper revised: June 9, 2022
Paper accepted: June 11, 2022